Naval Research Laboratory
Washington, DC 20375-5320

U.S. NAVAL RESEARCH LABORATORY

NRL/5610/MR—2024/1

Improvement in Scattered Light Rejection in Transmissometry Using Image Plane Vortex Phase Masks

SHAWN DIVITT

MATTHEW B. HART

VASANTHI SIVAPRAKASAM

ABBIE T. WATNIK

Optical Physics Branch
Optical Sciences Division

KYLE PETER JUDD

Applied Optics Branch
Optical Sciences Division

WILLIAM F. SPRUILL

TAREIK J. JACKSON

SEAP Intern
Washington, DC

January 16, 2024

REPORT DOCUMENTATION PAGE

PLEASE DO NOT RETURN YOUR FORM TO THE ABOVE ORGANIZATION

1. REPORT DATE	2. REPORT TYPE	3. DATES COVERED	
		START DATE	END DATE
16 -01-2024	NRL Memorandum Report	10/01/2020	12/31/2023

4. TITLE AND SUBTITLE

Improvement in Scattered Light Rejection in Transmissometry Using Image Plane Vortex Phase Masks

5a. CONTRACT NUMBER	5b. GRANT NUMBER	5c. PROGRAM ELEMENT NUMBER
5d. PROJECT NUMBER	**5e. TASK NUMBER**	**5f. WORK UNIT NUMBER**
		6C42

6. AUTHOR(S)

Shawn Divitt, Kyle P. Judd, Matthew B. Hart, William F. Spruill , Tareik, J. Jackson, Vasanthi Sivaprakasam, and Abbie T. Watnik

7. PERFORMING ORGANIZATION / AFFILIATION NAME(S) AND ADDRESS(ES)

Naval Research Laboratory
4555 Overlook Ave SW
Washington, DC 20375-5320

8. PERFORMING ORGANIZATION REPORT NUMBER

NRL/5610/MR—2024/1

9. SPONSORING / MONITORING AGENCY NAME(S) AND ADDRESS(ES)	10. SPONSOR / MONITOR'S ACRONYM(S) NUMBER	11. SPONSOR / MONITOR'S REPORT NUMBER(S)
Naval Research Laboratory 4555 Overlook Ave SW Washington, DC 20375-5320	NRL	

12. DISTRIBUTION / AVAILABILITY STATEMENT

DISTRIBUTION STATEMENT A: Approved for public release; distribution is unlimited.

13. SUPPLEMENTAL NOTES

14. ABSTRACT

We experimentally demonstrate a 14% improvement in coherent-to-incoherent power ratio in a laser transmissometer utilizing a pinhole spatial filter by augmenting it with a vortex phase mask and beam block combination.

15. SUBJECT TERMS

Transmissometry; Scattering mitigation; Vortex; Coronagraph

16. SECURITY CLASSIFICATION OF:			17. LIMITATION OF ABSTRACT	18. NUMBER OF PAGES
a. REPORT	b. ABSTRACT	c. THIS PAGE		
U	U	U	SAR	7

19a. NAME OF RESPONSIBLE PERSON	19b. PHONE NUMBER *(Include area code)*
Shawn Divitt	(484) 999-0347

This page intentionally left blank.

Improvement in Scattered Light Rejection in Transmissometry Using Image Plane Vortex Phase Masks

SHAWN DIVITT,[1,*] K. PETER JUDD,[1] MATTHEW B. HART,[1] WILLIAM F. SPRUILL,[1] TAREIK J. JACKSON II,[1] VASANTHI SIVAPRAKASAM,[1] AND ABBIE T. WATNIK [1]

[1] *Optical Sciences Division, U.S. Naval Research Laboratory, 4555 Overlook Ave. SW, Washington DC, 20375 USA*

[*] *shawn.divitt@nrl.navy.mil*

Abstract: We experimentally demonstrate a 14% improvement in coherent-to-incoherent power ratio in a laser transmissometer utilizing a pinhole spatial filter by augmenting it with a vortex phase mask and beam block combination.

1. Introduction

There has been significant recent interest in applying optical phase elements for separation of coherent and incoherent light, especially in the context of transmissometry through turbid media [1–6]. A challenge in turbid environments is measuring the transmission at high attenuation lengths, where eventually the signal is lost due to low throughput or is swamped by scattering. Previous results have shown that a optical vortex phase mask [1, 2, 7] or an axicon [3, 8] can be used to filter scattered or incoherent light, implying that these elements have applications in transmissometry.

Here, we show through experiment that the combination of a pinhole spatial filter and vortex phase mask, as described in theory elsewhere [6], can measure Beer's Law to greater attenuation lengths than shown previously. We also examine the benefit of the pinhole-vortex combination in relation to a pinhole alone, a vortex alone, and without any filtering other than the entrance pupil.

2. Experimental Details

We study the scatter-filtering ability of vortex phase masks using the setup shown in Fig. 1. A laser with wavelength 532 nm and average power of 4 W is expanded, collimated, and focused through a 4 ft (122 cm) long water tank using a lens (**L**, focal length 2 m, diameter 25 mm). Each side of the acrylic tank has an anti-reflection coated optical window, **w** (diameter 50 mm). After passing through the scattering fluid in the tank and a second window, the beam is returned

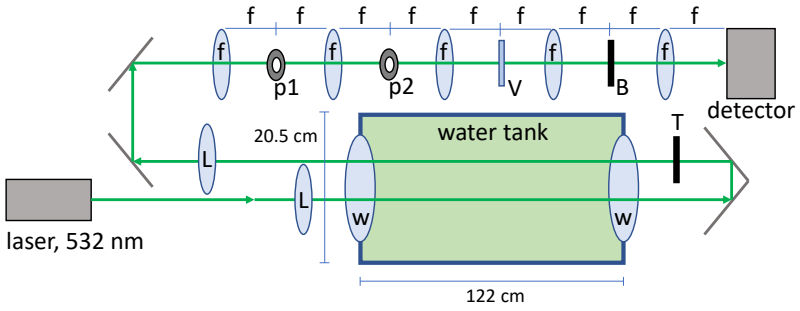

Fig. 1. A schematic diagram of the experimental setup (not to scale).

Manuscript approved January 16, 2024.

setup name	p1	p2	V	B
unfiltered		×		
vortex		×	×	×
pinhole	×	×		
vortex and pinhole (v + p)	×	×	×	×

Table 1. A table of optical elements present in the named setups. A × symbol indicates that the element is present.

through the tank for a second pass, using mirrors. The target/object to be imaged is placed at position **T**, just before entering the tank for the second time. A second lens **L** recollimates the laser light exiting the tank. The collimated beam is then passed through the optical system comprised of a set of lenses and other optical components before striking the plane array detector. The optical system is composed of four aspheric lenses (f, focal length 100 mm, diameter 50 mm), each separated by a distance of 2f in a Fourier transforming arrangement such that a laser focus can be found at the planes labelled **p1**, **V**, and on the detector, while a Fourier or pupil plane is located at the planes labelled **p2** and **B**. The various components **p1**, **V**, and **B** are inserted or removed to create different configurations of the optical system, where **p1** is an optical pinhole with diameter 50 μm, **p2** is an optical pinhole with diameter 1.00 mm and is always in place where it serves as the pupil of the system, **V** is a vortex phase mask with charge 2, and **B** is a circular metal beam block on glass (inverse pinhole) with diameter 1.08 mm. With **p2** in place and **p1**, **V**, and **B** removed, the optical system has an approximately 1.5 degree (full angle) field of view, found by considering the angular size of the leftmost tank window from the viewpoint of the first lens of the optical system.

We study the scatter-filtering ability of the various configurations of the optical system by adding plastic micro-particles to the water and measuring the power on the detector in conjunction with a target, **T**. We measure the attenuation length by passing light from a second, monitoring laser (not shown, wavelength 532 nm) through the side of the tank over a distance 20.5 cm and recording the transmitted power to determine the attenuation constant of the fluid. The fluid is

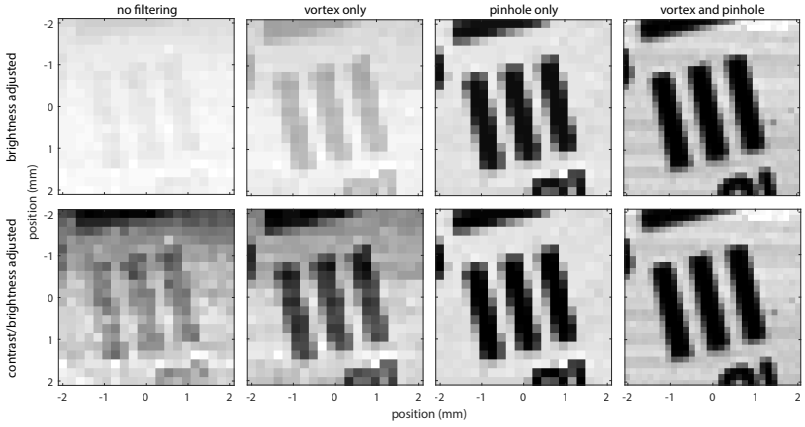

Fig. 2. Raster-scanned images recorded under the different configurations of the optical setup and under different image processing.

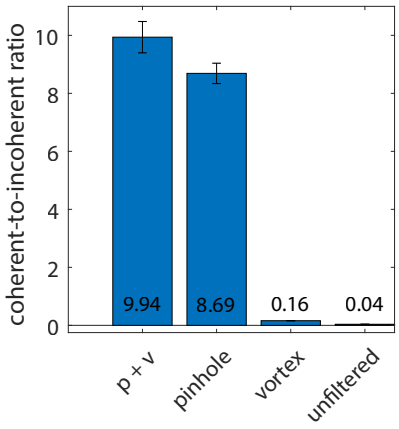

Fig. 3. The coherent-to-incoherent ratio achieved by the four listed configurations of the optical setup through a scattering fluid with 22.3 attenuation lengths of extinction.

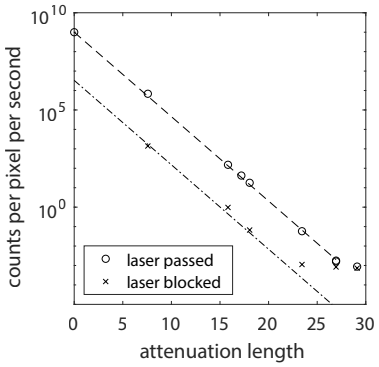

Fig. 4. A semi-log plot of the counts per pixel per second measured on the detector of the combined pinhole and vortex system versus the attenuation length measured using the monitoring laser. The dashed line represents Beer's Law adjusted to start at the clean-water count rate (attenuation length 0) with the laser allowed to pass through plane **T**. The dashed-dotted line represents Beer's Law adjusted to pass through the count rate at the point near 6 attenuation lengths with the laser blocked at plane **T**.

constantly and vigorously mixed using four fans inside the tank, not shown. Using the measured attenuation constant we can calculate the number of attenuation lengths expected over the long dimension of the tank by applying Beer's Law and comparing it to the values measured in the detector. We define Beer's Law as

$$I = I_0 \exp(-\alpha z) \tag{1}$$

where I is the remaining laser power after passing through the fluid, I_0 is the incident laser power before the fluid, α is the attenuation constant, and z is the total optical path length through the fluid. We define the attenuation length, a dimensionless quantity, as equal to the product αz.

To quantify the filtering ability of the different optical setup configurations, we make signal-on (laser passed) and signal-off (laser blocked) measurements where the focus at plane **T** is either completely transmitted or completely blocked, again with fluid attenuation length ($\alpha z = 22.3$)

and laser power (4 W). The vast majority of the scattering occurs in the fluid just after the laser enters the left window of the tank, as oriented in Fig. 1. The fluid in this region is thus the main source of scattering background that is present in the images of Fig. 2. Blocking the laser beam at plane **T** has negligible effect on the total scattered power received on the detector, especially at high attenuation lengths. Therefore we can find the ratio, r, of coherent (unscattered/ballistic) light to incoherent (scattered) light received on the detector by evaluating the following function:

$$r = \frac{u - b}{b} \tag{2}$$

where u is the power received on the detector when plane **T** is unblocked/transmissive and b is the power received on the detector when **T** is completely blocked. Since u measures the sum of coherent and incoherent power, and b measures only the incoherent power, r gives the ratio of coherent to incoherent power.

3. Results and Discussion

A set of representative images are shown in Fig. 2. The target is a single set of bars from a 1951 USAF bar target, composed of opaque metal on glass. The illumination is operated in a point-scanning mode where the target itself is raster-scanned through the focus of the beam at position **T** to create an image, with an exposure time of 200 ms and averaging with 4 exposures per position. For a 20×20 pixel image, the scan takes approximately 5 minutes. The columns in the figure are separated by the configurations of the optical system under the same fluid attenuation length ($\alpha z = 22.3$) and laser power (4 W) conditions. Table 1 is provided for reference, where a $\times$ indicates an element is present in the given setup configuration. In the "no filtering" column, only **p2** is inserted in the optical setup. In the "vortex only" column, **p2**, **V**, and **B** are inserted. In the "pinhole only" column, **p1**, and **p2** are inserted. In the "vortex and pinhole" column, **p1**, **p2**, **V**, and **B** are all inserted. The rows in the figure are separated by the applied image processing, where the top row is brightness-adjusted and the bottom row is both contrast- and brightness-adjusted. The top row visually shows the ratios of scattered and signal power, while the bottom row more effectively shows the shot noise associated those powers. By visual inspection, we find the image contrast increases from left to right, indicating that the vortex phase mask and beam block work to filter scattered light better than the entrance pupil alone, that the pinhole works better still, and that the combination of vortex and pinhole performed the best, although the difference in contrast between pinhole alone versus pinhole and vortex is not easily discernible by eye.

The results of representative signal-on versus signal-off experiments for each setup configuration are given in Fig. 3. For each of the two positions, laser passed or laser blocked at plane **T**, we gather 256 independent data points for noise-reduction purposes, with an exposure time of 200 ms per data point. At 22.3 attenuation lengths the coherent-to-incoherent power ratio on the detector is 0.04 in the unfiltered case (see Table 1), 0.16 in the vortex-only case, 8.69 in the pinhole-only case, and 9.94 in the pinhole and vortex combined case. These results are consistent with those expected by Watnik et al. [6]. The ratio in the combined case is about 14% larger than in the pinhole-only case, which agrees fairly well with the 2-10% expectation discussed in [6]. While the power ratio in [6] for the vortex-only case was 420 times greater than the unfiltered case, in the current work it is only 4 times greater. This discrepancy can be partially explained by the different fields of view of the unfiltered systems. The system in [6] had an 8 degree field of view, while the system in this work has a 1.5 degree field of view, and $8^2/1.5^2 \approx 28$, which means we would expect the power ratio in the vortex-only case to be about $4 \times 28 = 112$ if the current system had an 8 degree field of view. We attribute the remaining loss in ratio to non-ideal conditions including inverse pinhole (**B**) size and shape, vortex phase mask (**V**) imperfections, optical aberrations in the lenses, and misalignment.

A comparison of Beer's Law to the apparent intensity at the detector is given in Fig. 4, using the pinhole and vortex combined configuration to filter scattered light. Here, the tank is filled with clean water and then scattering particles are systematically added while power is recorded on the detector. The ∘ markers plot the counts per unit time received by the detector when the laser is allowed to pass through plane **T** while the × markers indicate the counts per second received by the detector when plane **T** is blocked. The counts per unit time are measured by taking into account the detector exposure time, integrated over a 100x100 pixel region of interest, and using 32 exposures per point to reduce random noise, keeping the gain fixed. A maximum exposure time of 750 ms per exposure was used, giving a maximum total exposure time of 24 seconds per point. Figure 4 shows that the "laser passed" case follows Beer's Law (dashed line) down to 26 attenuation lengths before levelling out due to noise, and the "laser blocked" case follows the same law (dashed-dotted line) to around 23 attenuation lengths. These plots indicate that the applied optical system is capable of measuring attenuation lengths up to 26 in a transmissometer mode, or alternatively that it can differentiate between signal-on and signal-off at up to 26 attenuation lengths in the presence of scatter under the conditions created in our particular water tank, with a noise floor at around 10^{-3} counts per pixel per second.

4. Conclusion

Here, we have experimentally demonstrated the use of a vortex phase mask and pinhole spatial filter in a transmissometer mode to filter scattered light. We found that images could be recorded with high contrast through at least 23 attenuation lengths of extinction due to a scattering fluid, that our optical system could differentiate between signal-on and signal-off at up to 26 attenuation lengths, and that the pinhole and vortex combination offered a 14% improvement in scattered-light filtering than a pinhole spatial filter alone.

Funding. US Naval Research Laboratory.

Disclosures. The authors declare no conflicts of interest.

Data availability. Data underlying the results presented in this paper are not publicly available at this time but may be obtained from the authors upon reasonable request.

References

1. B. Cochenour, L. Rodgers, A. Laux, L. Mullen, K. Morgan, J. K. Miller, and E. G. Johnson, "The detection of objects in a turbid underwater medium using orbital angular momentum (OAM)," in *Ocean Sensing and Monitoring IX,* vol. 10186 W. W. Hou and R. A. Arnone, eds., International Society for Optics and Photonics (SPIE, 2017), p. 1018603.
2. A. Jantzi, W. Jemison, A. Laux, L. Mullen, and B. Cochenour, "Enhanced underwater ranging using an optical vortex," Opt. express **26**, 2668–2674 (2018).
3. A. Jantzi, L. Rumbaugh, and W. Jemison, "Spatial coherence filtering for scatter rejection in underwater laser systems," in *Ocean Sensing and Monitoring XI,* vol. 11014 (SPIE, 2019), pp. 20–29.
4. A. Jantzi, W. Jemison, D. Illig, and L. Mullen, "Spatial and temporal domain filtering for underwater lidar," J. Opt. Soc. Am. A **38**, B10–B18 (2021).
5. B. Cochenour, A. Alley, A. E. Laux, and L. Mullen, "Optical vortex transmissometer," US Patent number US-11480522-B2. https://image-ppubs.uspto.gov/dirsearch-public/print/downloadPdf/11480522 (2022).
6. A. T. Watnik, S. Divitt, and M. Hart, "Separation of coherent and incoherent light using image plane vortex phase masks," J. Opt. Soc. Am. A **40**, 1372–1381 (2023).
7. G. A. Swartzlander Jr, "The optical vortex coronagraph," J. Opt. A: Pure Appl. Opt. **11**, 094022 (2009).
8. A. Jantzi, W. Jemison, D. Illig, and L. Mullen, "Axicons for improved lidar performance," in *Ocean Sensing and Monitoring XII,* vol. 11420 (SPIE, 2020), pp. 67–79.